

Mechanism and Substrate Recognition of 2-Hydroxyethylphosphonate Dioxygenase

Spencer C. Peck,^{†,‡} Heather A. Cooke,^{†,‡} Robert M. Cicchillo,[‡] Petra Malova,[§] Friedrich Hammerschmidt,[§] Satish K. Nair,^{||} and Wilfred A. van der Donk^{*,†,‡}

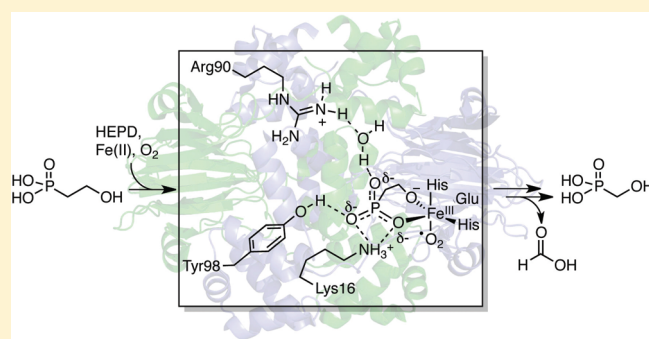
[†]Department of Chemistry and Howard Hughes Medical Institute and [‡]Institute for Genomic Biology, University of Illinois, 1206 West Gregory Drive, Urbana, Illinois 61801, United States

[§]Institute of Organic Chemistry, University of Vienna, Währingerstrasse 38, A-1090 Vienna, Austria

^{||}Department of Biochemistry and Center for Biophysics and Computational Biology, University of Illinois, Urbana, Illinois 61801, United States

S Supporting Information

ABSTRACT: HEPD belongs to the superfamily of 2-His-1-carboxylate non-heme iron-dependent dioxygenases. It converts 2-hydroxyethylphosphonate (2-HEP) to hydroxymethylphosphonate (HMP) and formate. Previously postulated mechanisms for the reaction catalyzed by HEPD cannot explain its conversion of 1-HEP to acetylphosphate. Alternative mechanisms that involve either phosphite or methylphosphonate as intermediates, which potentially explain all experimental studies including isotope labeling experiments and use of substrate analogues, were investigated. The results of these studies reveal that these alternative mechanisms are not correct. Site-directed mutagenesis studies of Lys16, Arg90, and Tyr98 support roles of these residues in binding of 2-HEP. Mutation of Lys16 to Ala resulted in an inactive enzyme, whereas mutation of Arg90 to Ala or Tyr98 to Phe greatly decreased $k_{\text{cat}}/K_{\text{m},2\text{-HEP}}$. Furthermore, the latter mutants could not be saturated in O_2 . These results suggest that proper binding of 2-HEP is important for O_2 activation and that the enzyme uses a compulsory binding order with 2-HEP binding before O_2 . The Y98F mutant produces methylphosphonate as a minor side product providing indirect support for the proposal that the last step during catalysis involves a ferric hydroxide reacting with a methylphosphonate radical.



Bioactive natural product phosphonates and phosphinates are widely employed in medicine and agriculture.¹ One example of this class of molecules is phosphinothricin (PT), which is the active ingredient in a number of commercially important herbicides.^{2,3} Recent investigations into the PT biosynthetic pathway revealed a number of previously uncharacterized transformations, including an unusual carbon–carbon bond cleavage during the conversion of 2-hydroxyethylphosphonate (2-HEP) to hydroxymethylphosphonate (HMP) and formate catalyzed by 2-hydroxyethylphosphonate dioxygenase (HEPD) (Scheme 1).^{4,5} HMP is then further elaborated to provide PT tripeptide in 15 enzymatic transformations.⁴

Biochemical and structural characterization of HEPD has shown that it is a mononuclear non-heme Fe(II)-dependent dioxygenase that does not require an external source of electrons such as α -ketoglutarate. The use of labeled substrates (2-HEP isotopologues, $^{18}\text{O}_2$, and $\text{H}_2\text{ }^{18}\text{O}$) showed that one of the atoms of dioxygen ends up in formate.⁵ The second oxygen atom is incorporated into the hydroxyl group of HMP in a substoichiometric fashion, as some of the oxygen exchanges with solvent.⁵ Surprisingly, experiments with 2-HEP that was stereospecifically labeled with deuterium at C1 demonstrated that the HMP

produced was racemic (Scheme 1).⁶ Several mechanisms that can explain the results of these labeling studies have been proposed recently,^{6,7} but these mechanisms do not explain why HEPD converts the substrate analogue 1-HEP to acetylphosphate, which could be the result of a Criegee rearrangement (Scheme 1).⁸ In this study, we examined several alternative mechanisms that could account for all experimental observations thus far. Additionally, we introduced mutations at residues responsible for binding 2-HEP in the active site of HEPD in the hopes that these active site mutants might perturb the chemistry of HEPD and provide a glimpse into the catalytic cycle.

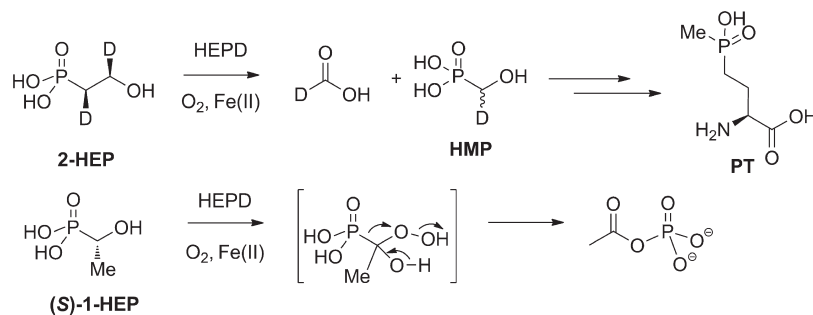
■ MATERIALS AND METHODS

Materials. 2-Nitrophenylhydrazine was obtained from Acros Organics. *N*-[3-(Dimethylamino)propyl]-*N'*-ethylcarbodiimide was purchased from Chem-Impex. NAP-5 and NAP-25 columns

Received: May 24, 2011

Revised: June 26, 2011

Published: June 28, 2011

Scheme 1. HEPD Requires Only Ferrous Iron and O₂ To Convert 2-HEP to HMP^a

^a The enzyme abstracts the *pro-S* hydrogen from C2, and all stereochemical information about C1 is lost in the product HMP. HEPD also converts (S)-1-HEP to acetylphosphate, possibly via a Criegee intermediate as shown.

were purchased from GE Healthcare. All other materials were purchased from Sigma Aldrich unless otherwise noted.

Mutagenesis. Site-directed mutagenesis was performed using the QuikChange mutagenesis kit (Stratagene). Primer sequences are available in the Supporting Information.

Protein Preparation. HEPD was expressed and purified as previously described.⁵ For kinetic assays, HEPD was further purified by size exclusion chromatography (Superdex 200 preparative grade resin, GE Healthcare). In a typical reconstitution, HEPD (70–200 μM for O₂ kinetics, up to 1 mM for ³¹P NMR assays) was anaerobically incubated with Fe(II) [1 equiv of (NH₄)₂Fe(SO₄)₂·6H₂O] on ice for at least 10 min in 25 mM HEPES (pH 7.5). All assays were performed in air-saturated 25 mM HEPES (pH 7.5) at 20 °C unless otherwise described.

Kinetic Assays. A Hansatech O₂ electrode was used to generate Michaelis–Menten curves by varying one substrate concentration while keeping the second substrate at saturating concentrations (when possible) and at a constant HEPD concentration (2 μM for the wild type, 5 μM for R90K and Y98F, and 10 μM for R90A; 25 μM K16A was used to ensure no activity was observed for this inactive mutant at higher enzyme concentrations). All reactions were initiated by addition of 2-HEP. The initial rate of O₂ consumption was measured in triplicate and normalized for the enzyme concentration. Nonlinear regressions were calculated using Igor Pro version 6.1.

Liquid Chromatography–Mass Spectrometry (LC–MS) Assays. Formate production assays were conducted as previously described.⁸ LC–MS analysis of phosphonate compounds was conducted using a hydrophilic interaction chromatography column (SeQuant ZIC-HILIC, 2.1 mm × 150 mm) followed by direct infusion onto a linear ion-trap/Fourier-transform hybrid mass spectrometer.

NMR Spectroscopy Assays. ³¹P NMR spectra were recorded on a Varian Unity Inova 600 spectrometer tuned to 242.79 MHz and referenced to an external standard (85% H₃PO₄, $\delta = 0$). For analysis of enzymatic products by NMR spectroscopy, reconstituted protein (100 μM) was added to 2-HEP (0.5–2 mM) in oxygenated buffer. After incubation for 1–2 h, EDTA (50 mM), dithionite (20 mM), and D₂O [final concentration of 20% (v/v)] were added, and the spectrum was recorded. Because of the sensitivity of chemical shifts recorded by ³¹P NMR spectroscopy to small changes in pH, the identity of all products was confirmed by spiking with authentic synthetic compounds. Spectra were plotted with MestReNova-Lite.

Size Exclusion Chromatography. All size exclusion chromatographic experiments were conducted with an isocratic gel

filtration buffer [200 mM KCl, 50 mM HEPES (pH 7.5), and 10% glycerol]. Analytical size exclusion chromatography was conducted at 20 °C with a flow rate of 1.0 mL/min on an HPLC Gel Filtration BioSil-250 column. Analytes were typically run at concentrations of 20–100 μM with 20 μL injections. Standards were bovine serum albumin, yeast alcohol dehydrogenase, β -amylase, carbonic anhydrase from bovine erythrocytes, and cytochrome *c* oxidase from horse heart. Blue dextran was used to determine the void volume. The elution volume (V_e) was divided by the void volume (V_0), and the parameter V_e/V_0 was correlated to the log of the molecular weight of the protein to construct a calibration curve.

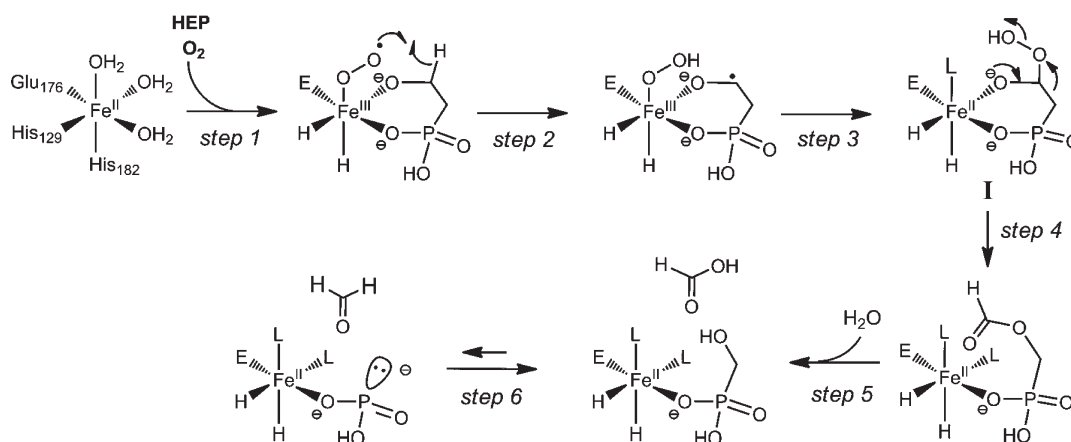
Determination of the Crystal Structure of Y98F. A crystal of the HEPD-Y98F mutant, from which the His₆ tag had been removed with thrombin, was obtained as previously reported for wild-type HEPD.⁵ A 6-fold redundant data set was collected from a crystal of HEPD-Y98F on a Mar 300 CCD detector (LSCAT, Sector 21 ID-D, Advanced Photon Source, Argonne, IL). Data were indexed and scaled using the HKL2000 package⁹ as summarized in Table S1 of the Supporting Information. The structure was determined via molecular replacement with apo-HEPD [Protein Data Bank (PDB) entry 3G7D] as the search model using MOLREP¹⁰ in the CCP4 suite.¹¹ Model building and refining were performed with COOT.¹² Refinement cycles and generation of electron density maps were accomplished with the CNS suite of programs¹³ until the R values no longer improved. PyMOL (DeLano Scientific, San Carlos, CA) was used to generate graphic images. The root-mean-square deviation between the mutant and wild-type HEPD was calculated via structural comparison using TopMatch.^{14,15}

RESULTS

Racemization of HMP Does Not Occur after Its Initial Formation. Previously proposed mechanisms for the conversion of 2-HEP to HMP and formate do not provide a satisfactory explanation for racemization both at C1 in the conversion of 2-HEP to HMP⁶ and the production of acetylphosphate from the substrate analogue 1-HEP⁸ (Scheme 1). On the basis of precedent in organic chemistry,¹⁴ the latter product suggests the involvement of a Criegee rearrangement from a hydroperoxylation product, but such rearrangements result in retention of stereochemistry. One model that would be consistent with the outcome of both previous studies is shown in Scheme 2.

In this mechanism, a hydroperoxylation process is followed by a Criegee rearrangement (step 4) and hydrolysis to form HMP

Scheme 2. Reversible Formation of Phosphite and Formaldehyde from HMP in the Active Site of HEPD Could Account for the Observed Racemization at C1

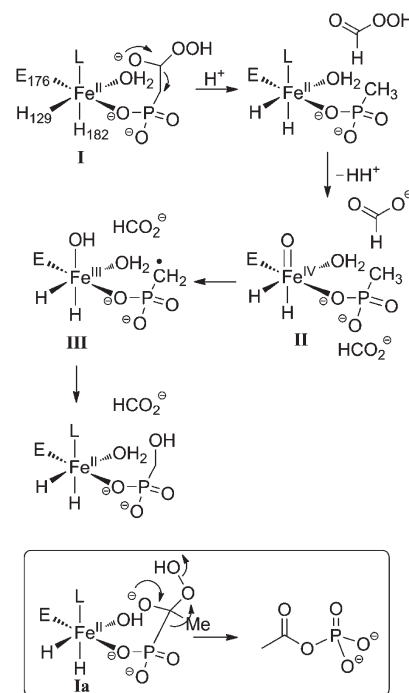


(step 5), as previously proposed.⁸ After formation of HMP, the P–C bond in the product could be transiently broken, generating phosphite and formaldehyde in the active site of HEPD (step 6). If the formaldehyde is able to rotate along the C=O bond, then phosphite could attack either face of the carbonyl group resulting in a loss of stereochemistry. In an effort to test this possibility, (*R*)-[²H₁]HMP^{6,15} was incubated with HEPD under anaerobic conditions. Subsequently, the solution was sparged with oxygen to effect the slow but stereospecific conversion of HMP to phosphate and formate.⁶ If the (*R*)-[²H₁]-HMP had (partially) racemized, then deuterium would be incorporated into formate to the same extent that racemization occurred. However, analysis of the formate by LC–MS after derivatization⁸ did not show any deuterium incorporation, and hence, the experiment provided no evidence of racemization of (*R*)-[²H₁]HMP.

Investigation of a Potential Methylphosphonate Intermediate. Another possible mechanism that could account for the production of racemic HMP from (*R*)- or (*S*)-2-[1-²H₁]HEP as well as the generation of acetylphosphate from 1-HEP is shown in Scheme 3. In this model, hydroperoxylation product **I**, generated as in Scheme 2, would undergo C–C bond cleavage to produce performic acid and methylphosphonate (MPn), an intermediate from which all stereochemical information would be lost. On the basis of literature precedent with model compounds,¹⁶ the performic acid could oxidize the iron to the corresponding ferryl species **II**, which could abstract a hydrogen atom from MPn. Rebound of the ferric hydroxide and the organic radical would generate the HMP product and reset the enzyme for another turnover. This mechanism could also explain the formation of acetylphosphate from 1-HEP if the hydroperoxylated intermediate **Ia** generated with this substrate analogue were to undergo a Criegee rearrangement instead of formation of peracetic acid (inset of Scheme 3).

Prima facie, the mechanism in Scheme 3 appears to be inconsistent with the previously observed retention of both deuterium atoms in HMP after oxidation of 2-[1-²H₂]HEP by HEPD.⁵ The mechanism in Scheme 3 would predict incorporation of a proton from solvent in methylphosphonate, and at least partial retention of this proton in the final product. However, hydrogen atom abstractions by ferryl species have been reported to result in large deuterium kinetic isotope effects (KIEs) of

Scheme 3. Formation of an Achiral Methylphosphonate Intermediate Could Explain the Racemization of HMP^a



^a Alternative breakdown of peroxyacetal **Ia** formed with 1-HEP would also explain the formation of acetylphosphate with this substrate analogue.

50–60 in TauD¹⁷ and prolyl-4-hydroxylase.¹⁸ A similarly strong discrimination against the abstraction of deuterium from [CHD₂]-MPn by ferryl intermediate **II** in HEPD would account for retention of both deuterium atoms in HMP because the sensitivity of the assay used would not be sufficient to detect <5% monodeuterated HMP. If the mechanism in Scheme 3 is operational with a large KIE, then an experiment performed with unlabeled 2-HEP in D₂O should produce monodeuterated HMP (Scheme 4).

Therefore, HEPD was incubated with 2-HEP in buffer prepared in D₂O (>99.8% D-labeled), and the HMP generated was

Scheme 4. Conversion of 2-HEP to Formate and HMP in D₂O Would Result in [²H₁]HMP If Methylphosphonate Were an Intermediate

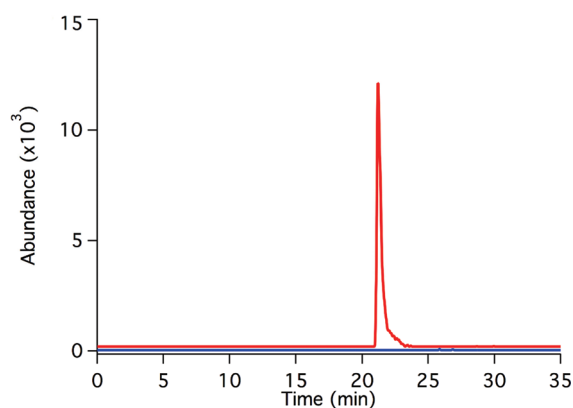
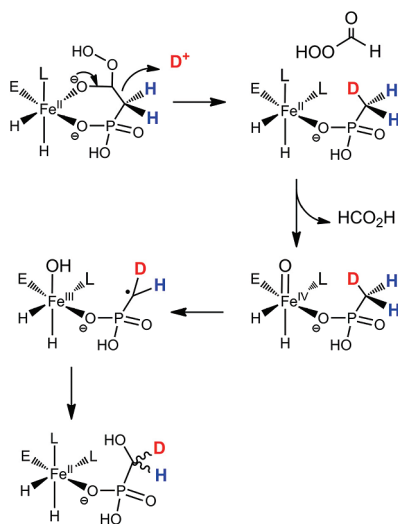


Figure 1. Extracted ion chromatograms (EIC) of reaction mixtures of 2-HEP incubated with wild-type HEPD in D₂O. [¹H₂]HMP was observed (red, calculated *m/z* 110.9847, found *m/z* 110.9852), but [²H₁]HMP (blue) was not detected.

analyzed by liquid chromatography–Fourier transform mass spectrometry (LC–FTMS). Extracted ion chromatograms were obtained using a linear ion-trap Fourier transform hybrid mass spectrometer allowing a 10 ppm mass error with respect to the theoretical masses. This method can distinguish between [²H₁]–HMP and other analytes such as natural abundance [¹³C]HMP. No [²H₁]HMP was detected (Figure 1), indicating that the mechanism in Scheme 4 cannot be correct. Although not discussed here in detail, this result also rules out a hydroxylation mechanism with a methylphosphonate intermediate (see Scheme S1 of the Supporting Information).

Mutagenesis of Substrate Binding Residues. Inspection of the cocrystal structure of 2-HEP bound to HEPD in which Cd(II) occupied the iron binding site led to the identification of several residues that appear to be involved in substrate binding (Figure 2). Several mutants of these residues were generated to investigate the importance of these residues for catalysis with the motivation that it might be possible to perturb the chemistry

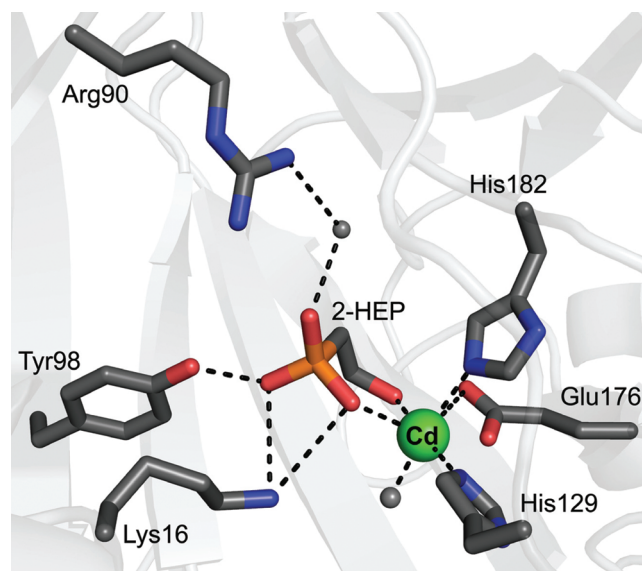


Figure 2. View of the active site of Cd(II)-substituted HEPD with 2-HEP bound. The 2-His-1-carboxylate triad binds Cd(II), to which 2-HEP coordinates in a bidentate fashion. Lys16, Arg90, and Tyr98 form part of a hydrogen bonding network that anchors 2-HEP in the active site.

performed by HEPD and thereby glean insight into the mechanism. To allow comparison of their kinetic parameters with those of the wild-type (wt) enzyme, a continuous steady state kinetics assay was developed using an oxygen electrode. Wild-type HEPD demonstrated a typical hyperbolic dependence on the concentrations of both 2-HEP and O₂ (Figure 3 and Figure S1 of the Supporting Information). Michaelis–Menten curves with the concentration of one substrate being varied and that of the second substrate being held at a saturating level allowed determination of the *K_m* values for both substrates as well as *k_{cat}* for wt HEPD (Figure 3 and Table 1). In the X-ray structure, Arg90 interacts with the phosphonate moiety of 2-HEP through an intermediate water molecule (Figure 2). Site-directed mutagenesis afforded the R90A mutant, which was shown by ³¹P NMR spectroscopy and LC–MS to convert 2-HEP to HMP and formate (Figures S2 and S3 of the Supporting Information). Analysis of the kinetics of the reaction using the oxygen electrode assay showed that the mutation resulted in a much higher apparent *K_m* for 2-HEP compared to that of wt HEPD (Figure 3). Because the R90A mutant could not be saturated in O₂ (Figure S1 of the Supporting Information), individual values for *K_{m,O2}* and *k_{cat}* could not be determined. From the observed rates at various oxygen concentrations, a value of $100 \pm 1 \text{ M}^{-1} \text{ s}^{-1}$ could be estimated for *k_{cat}/K_{m,O2}*. The R90K mutant was also constructed and shown to convert 2-HEP to HMP and formate by ³¹P NMR spectroscopy and LC–MS (Figures S2 and S3 of the Supporting Information), respectively. Its *K_m* for 2-HEP was increased compared to that of wt HEPD but not as significantly as observed for R90A (Table 1). Under O₂ saturating conditions, the calculated *k_{cat}* of the R90K mutant is comparable to that of wt, demonstrating that the mutation of Arg to Lys provided full HEPD activity at higher 2-HEP concentrations.

A tyrosine-lysine pair crucial for substrate binding has been observed in several enzymes involved in phosphonate biosynthesis, including HppE involved in fosfomycin biosynthesis and the *O*-methyltransferase DhpI involved in the biosynthesis of dehydrophos.^{20–22} In HEPD, Lys16 and Tyr98 constitute this

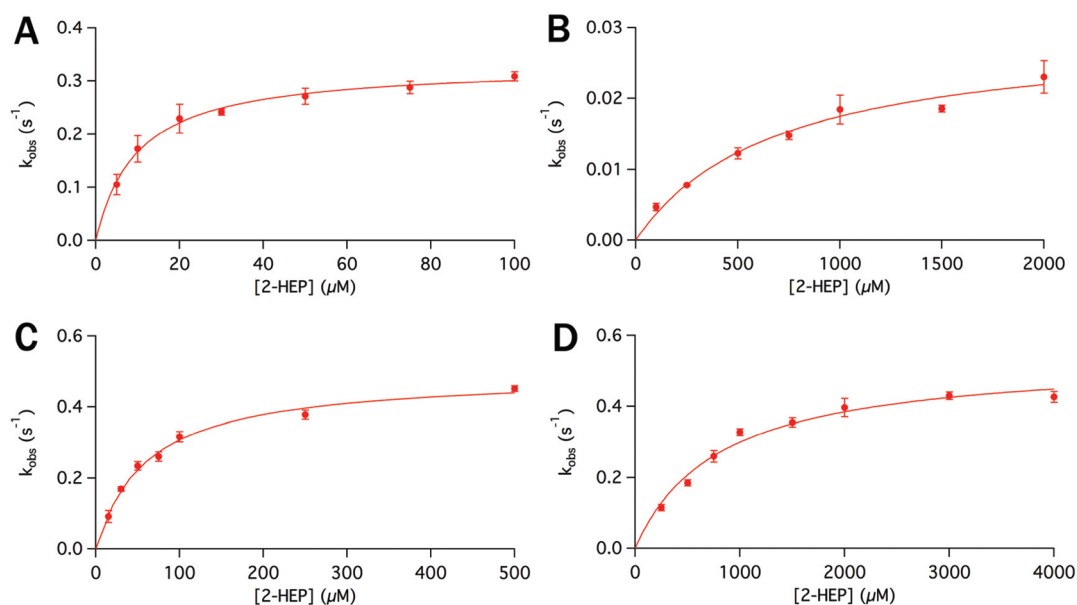


Figure 3. Kinetics of oxidation of 2-HEP by HEPD: (A) wt, (B) R90A, (C) R90K, and (D) Y98F. All data were obtained with air-saturated buffer.

Table 1. Kinetic Parameters of HEPD and Its Variants

HEPD	k_{cat} (s^{-1})	$K_{\text{m},2\text{-HEP}}$ (μM)	$k_{\text{cat}}/K_{\text{m},2\text{-HEP}}$ ($\text{M}^{-1} \text{s}^{-1}$)	K_{m,O_2} (μM)	$k_{\text{cat}}/K_{\text{m},\text{O}_2}$ ($\text{M}^{-1} \text{s}^{-1}$)
wild type	0.35 ± 0.01	9.8 ± 1	$(3.6 \pm 0.3) \times 10^4$	33 ± 1	$(11 \pm 0.02) \times 10^3$
R90A	N/A ^b	690 ± 140^a	N/A ^b	N/A ^b	100 ± 1
R90K	0.81 ± 0.01^c	60 ± 6	$(1.3 \pm 0.1) \times 10^4$	100 ± 1	$(8.1 \pm 0.04) \times 10^3$
K16A	inactive	inactive	inactive	inactive	inactive
Y98F	N/A ^b	800 ± 110^a	N/A ^b	N/A ^b	740 ± 30

^a Apparent K_{m} value. ^b Could not be obtained as these mutants could not be saturated in O_2 (see the text). ^c See Figure S1C.

pair of residues (Figure 2). In the cocrystal structure of HEPD with 2-HEP, Lys16 protrudes from one monomer into the active site of the other monomer to interact with the phosphonate moiety of 2-HEP. To probe the importance of this residue, the K16A mutant was constructed. Consistent with the findings for similar mutants of DhpI¹⁹ and HppE,²¹ the lysine to alanine substitution completely abolished activity. To examine whether this inactivation was a consequence of the abolition of a vital electrostatic interaction with the substrate or disruption of the dimer interface, analytical gel filtration was performed on the mutant and wt enzyme. Both the wt apoenzyme and the enzyme reconstituted with Fe(II) eluted as dimers, and the elution profiles of K16A could be superimposed with those of wt HEPD, indicating that Lys16 likely forms an electrostatic interaction that is critical for binding 2-HEP in the active site of HEPD.

In the Cd(II)–HEPD crystal structure without substrate, the phenolic oxygen of Tyr98 points away from the active site. When 2-HEP was cocrystallized with HEPD, Tyr98 was observed to undergo a substantial torsional rotation to move the phenolic oxygen toward the phosphonate moiety of 2-HEP. To investigate the importance of Tyr98 for catalysis, we generated the Y98F mutant. The mutant still converted 2-HEP to HMP and formate as observed by ³¹P NMR spectroscopy and LC–MS (Figures S2 and S3 of the Supporting Information), but in contrast to that of wt HEPD, which consumed O_2 without a loss of catalytic activity, the rate of consumption of O_2 by HEPD–Y98F gradually decreased until the enzyme had lost all activity well before

substrate had been consumed (Figure S4 of the Supporting Information); addition of more substrate or reductant did not result in reactivation of the mutant. Inactivation was sufficiently slow that kinetic parameters could be determined (Figure 3 and Table 1). Characterization of the Michaelis–Menten kinetics using the oxygen electrode assay demonstrated a large increase in the apparent $K_{\text{m},2\text{-HEP}}$, and like that of R90A, the rate of catalysis by Y98F could not be saturated in O_2 (Figure S1 of the Supporting Information).

To further investigate the slow inactivation of Y98F, we analyzed the products via LC–FTMS, a technique that is more sensitive than ³¹P NMR spectroscopy. Low levels of MPn (Figure S5 of the Supporting Information) were detected, which was not observed with wt HEPD or the other mutants. Like MPn detected in the assay, MPn authentic standards were consistently detected as dimers (theoretical mass of m/z 190.9874, found mass of m/z 190.9877). To determine the origin of the additional hydrogen on the methyl group of MPn, Y98F was incubated with 2-HEP in D_2O . No incorporation of deuterium into MPn was observed (Figure 4), suggesting the intermediacy of an MPn radical rather than an MPn anion.

To investigate whether the mutation had caused any substantial changes to the active site, the crystal structure of the Y98F mutant was determined (Figure 5). Comparison with the structure of wt HEPD shows that the loss of the phenolic oxygen does not substantially perturb the overall structure [root-mean-square deviation of C α atoms of 0.3 Å compared to Cd(II)-bound

HEPD]. Furthermore, the arrangement of the active site of Y98F is very similar to that of the wild type. The phenylalanine residue

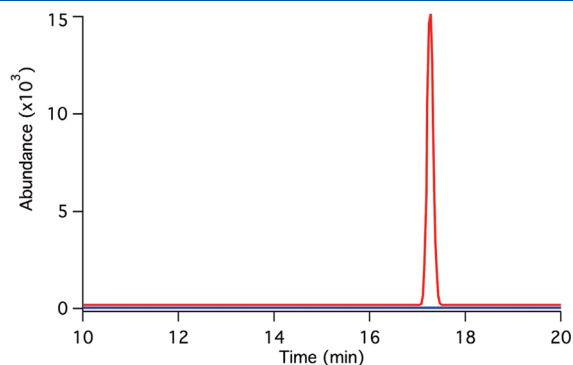


Figure 4. EICs of reaction mixtures of HEPD-Y98F with 2-HEP in D_2O . Only protiated MPn (red, found mass of m/z 190.9877, calculated mass of m/z 190.9874 for the $[MPn]_2^-$ dimer) was observed, and deuterium-labeled MPn (blue) was not detected (within a 10 ppm mass error).

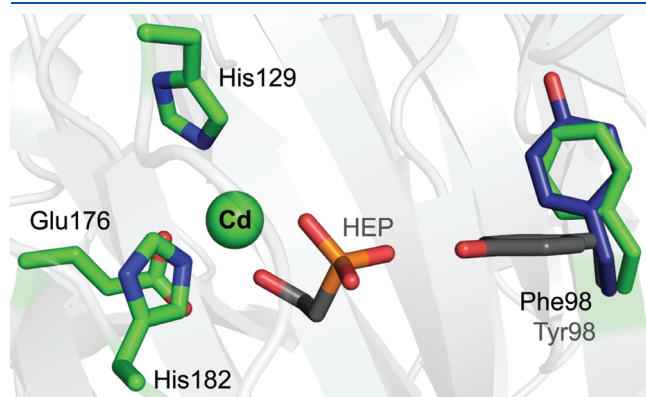


Figure 5. Overlay of apo-HEPD, HEPD with 2-HEP bound, and HEPD-Y98F. Iron-binding residues, Cd(II), and Phe98 are colored green and are from the mutant structure (PDB entry 3RZZ). Colored gray are 2-HEP and Tyr98 from the liganded wt HEPD structure (PDB entry 3GBF). Colored blue is Tyr98 from apo-HEPD (PDB entry 3G7D). Tyr98 undergoes a torsional rotation into the active site as a result of a hydrogen bond that forms between the phenolic oxygen of tyrosine and a phosphonate oxygen of 2-HEP.

points away from the active site as in the apo-HEPD structure, and without the phenolic oxygen, it is unlikely that the phenylalanine would rotate toward the active site upon 2-HEP binding. Attempts to determine a cocrystal structure were unsuccessful, underscoring again the importance of the Y98 residue for binding of 2-HEP.

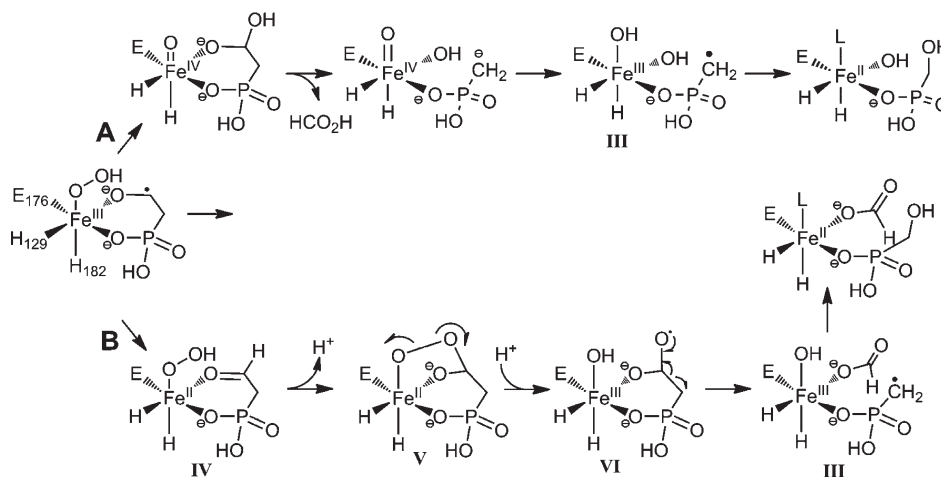
DISCUSSION

The recent finding that the stereochemical information about C1 of 2-HEP is lost during its conversion to HMP by HEPD required revision of the originally proposed mechanisms.⁵ Several new mechanistic scenarios were suggested,^{6–8} but none could provide a rationale for how the substrate analogue 1-HEP is converted to acetylphosphate by HEPD. In this work, we evaluated two new mechanisms that, if operative, could explain both the loss of stereochemistry and the apparent involvement of a Criegee rearrangement, and hence the intermediacy of a hydroperoxylation product. However, experimental tests of these new mechanisms argue against both scenarios. We therefore are left with the conclusion that the substrate analogue 1-HEP induces alternative chemistry, which is not unusual for non-heme iron-dependent enzymes (e.g., refs 20–22)

For the reaction with the native substrate 2-HEP, two mechanisms can account for all experimental observations (Scheme 5). The results with the R90A and Y98F mutants provide experimental support that 2-HEP binds prior to dioxygen because the enzyme could be saturated in 2-HEP but not O_2 . The latter observation suggests that the Arg90 and Tyr98 residues are important not only for binding of 2-HEP but also for orienting the substrate such that it activates the Fe(II) ion for O_2 binding. Bidentate binding of substrate has been suggested previously to facilitate oxygen activation.^{5,21,22} The results reported here for Arg90, Lys16, and Tyr98 mutants also illustrate the importance of these residues for phosphonate binding as the apparent $K_{m,2-HEP}$ values increased greatly for the R90A and Y98F mutants whereas the K16A mutant was entirely inactive.

After oxygen binding, the resulting ferric superoxo species is postulated to abstract the *pro-S* hydrogen atom from C2 of 2-HEP to generate a substrate radical as shown in Scheme 5. The intermediate radical is then hydroxylated (pathway A) or undergoes a one-electron transfer to the iron to generate an aldehyde IV (pathway B).

Scheme 5. Two Mechanisms That Can Account for the Observed Experimental Outcomes during 2-HEP Oxidation



In pathway A, C–C bond cleavage generates an anion that is oxidized to radical **III**, at which point the stereochemistry may be lost. Rebound with the ferric hydroxide then provides HMP. Exchange of either the ferryl or ferric hydroxide intermediates with solvent can account for the observed incorporation of oxygen derived from solvent into HMP.⁵ In pathway B, favored by DFT calculations,⁷ a bridged peroxy intermediate **V** is formed in which the O–O bond is cleaved homolytically to generate a ferric hydroxide and radical **VI**, which undergoes β -scission to generate the same methylphosphonate radical **III** as in pathway A. This radical can then combine with the ferric hydroxide to generate HMP and reset the enzyme for another turnover. Once more, solvent exchange of the ferric hydroxide can account for incorporation of oxygen from solvent into HMP.

The observation that during inactivation of Y98F the hydrogen in MPn is not derived from solvent provides additional indirect support for the mechanisms shown in Scheme 5. Given the short distance (2.32 Å) between the phenolic oxygen of Tyr98 and one of the oxygens of the phosphonate group of 2-HEP in the X-ray structure of wt HEPD, the loss of this hydrogen bond in the Y98F mutant may result in a less well-defined binding conformation of the substrate during catalysis. In turn, this may result in suboptimal arrangement of radical **III** with respect to the ferric hydroxide for rebound, resulting in abstraction of a hydrogen atom from the protein that initiates irreversible inactivation.

In summary, these data rule out the presence of phosphite or methylphosphonate intermediates that would account for the observed loss of stereochemical information about C1 of 2-HEP. On the basis of the crystal structure of HEPD, three residues that are crucial for anchoring the phosphonate moiety of 2-HEP during catalysis were identified, and their importance was confirmed via characterization of the oxidation kinetics of various site-directed mutants. These mutational studies have led us to the conclusion that the mechanism of HEPD involves a compulsory binding order with substrate binding triggering O₂ binding and subsequent activation for catalysis. Moreover, analysis of the chemistry of the Y98F mutant indicates that the last step is likely ferric hydroxide rebound with an MPn radical.

■ ASSOCIATED CONTENT

S Supporting Information. Primers used for site-directed mutagenesis, an alternative mechanism that invokes the intermediacy of methylphosphonate, plots showing the dependence of rates on O₂ concentration, NMR and MS analysis of the products of HEPD mutants, and refinement statistics for the HEPD-Y98F crystal structure. This material is available free of charge via the Internet at <http://pubs.acs.org>.

■ AUTHOR INFORMATION

Corresponding Author

*Telephone: (217) 244-5360. Fax: (217) 244-8533. E-mail: vddonk@illinois.edu.

Funding Sources

This work was supported by the National Institutes of Health (GM077596 to W.A.v.d.D.). S.C.P. is a trainee in the Chemistry-Biology Interface Training Program (T32 GM070421). H.A.C. holds a National Institutes of Health NRSA Postdoctoral Fellowship (F32 GM95024-01).

■ ACKNOWLEDGMENT

We thank Drs. Bradley Evans and Changming Zhao for help with LC–FTMS analysis.

■ ABBREVIATIONS

PT, phosphinothricin; 2-HEP, 2-hydroxyethylphosphonate; HMP, hydroxymethylphosphonate; HEPD, 2-hydroxyethylphosphonate dioxygenase; MPn, methylphosphonate; EIC, extracted ion chromatogram; wt, wild-type; HppE, hydroxypropylphosphonate epoxidase.

■ REFERENCES

- (1) Metcalf, W. W., and van der Donk, W. A. (2009) Biosynthesis of Phosphonic and Phosphinic Acid Natural Products. *Annu. Rev. Biochem.* 78, 65–94.
- (2) Bayer, E., Gugel, K. H., Hägele, K., Hagenmaier, H., Jessipow, S., König, W. A., and Zähler, H. (1972) Stoffwechselprodukte von Mikroorganismen 98. Mitteilung. Phosphinothricin und phosphinothricylalanyl-alanin. *Helv. Chim. Acta* 55, 224–239.
- (3) Thompson, C. J., and Seto, H. (1995) Bialaphos. *Biotechnology* 28, 197–222.
- (4) Blodgett, J. A., Thomas, P. M., Li, G., Velasquez, J. E., van der Donk, W. A., Kelleher, N. L., and Metcalf, W. W. (2007) Unusual transformations in the biosynthesis of the antibiotic phosphinothricin tripeptide. *Nat. Chem. Biol.* 3, 480–485.
- (5) Cicchillo, R. M., Zhang, H., Blodgett, J. A. V., Whitteck, J. T., Li, G., Nair, S. K., van der Donk, W. A., and Metcalf, W. W. (2009) An unusual carbon-carbon bond cleavage reaction during phosphinothricin biosynthesis. *Nature* 459, 871–874.
- (6) Whitteck, J. T., Malova, P., Peck, S. C., Cicchillo, R. M., Hammerschmidt, F., and van der Donk, W. A. (2011) On the stereochemistry of 2-hydroxyethylphosphonate dioxygenase. *J. Am. Chem. Soc.* 133, 4236–4239.
- (7) Hirao, H., and Morokuma, K. (2010) Ferric Superoxide and Ferric Hydroxide Are Used in the Catalytic Mechanism of Hydroxyethylphosphonate Dioxygenase: A Density Functional Theory Investigation. *J. Am. Chem. Soc.* 132, 17901–17909.
- (8) Whitteck, J. T., Cicchillo, R. M., and van der Donk, W. A. (2009) Hydroperoxylation by hydroxyethylphosphonate dioxygenase. *J. Am. Chem. Soc.* 131, 16225–16232.
- (9) Otwinowski, Z., and Minor, W. (1997) Processing of X-ray diffraction data collected in oscillation mode. *Methods Enzymol.* 276, 307–326.
- (10) Vagin, A., and Teplyakov, A. (1997) MOLREP: An automated program for molecular replacement. *J. Appl. Crystallogr.* 30, 1022–1025.
- (11) Bailey, S. (1994) The CCP4 Suite: Programs for Protein Crystallography. *Acta Crystallogr. D50*, 760–763.
- (12) Emsley, P., and Cowtan, K. (2004) Coot: Model-building tools for molecular graphics. *Acta Crystallogr. D60*, 2126–2132.
- (13) Brunger, A. T. (2007) Version 1.2 of the Crystallography and NMR system. *Nat. Protoc.* 2, 2728–2733.
- (14) Gordon, N. J., and Evans, S. A., Jr. (1993) Acyl phosphates from acyl phosphonates: A novel Baeyer-Villiger rearrangement. *J. Org. Chem.* 58, 4516–4519.
- (15) Kapeller, D., Barth, R., Mereiter, K., and Hammerschmidt, F. (2007) Preparation of chiral α -oxy-²H₁]methylolithiums of 99% ee and determination of their configurational stability. *J. Am. Chem. Soc.* 129, 914–923.
- (16) Lim, M. H., Rohde, J.-U., Stubna, A., Bukowski, M. R., Costas, M., Ho, R. Y. N., Münck, E., Nam, W., and Que, L., Jr. (2003) An Fe(IV)O complex of a tetradentate tripodal nonheme ligand. *Proc. Natl. Acad. Sci. U.S.A.* 100, 3665–3670.
- (17) Price, J. C., Barr, E. W., Glass, T. E., Krebs, C., and Bollinger, J. M., Jr. (2003) Evidence for hydrogen abstraction from C1 of taurine by the high-spin Fe(IV) intermediate detected during oxygen activation by

taurine: α -ketoglutarate dioxygenase (TauD). *J. Am. Chem. Soc.* **125**, 13008–13009.

(18) Hoffart, L. M., Barr, E. W., Guyer, R. B., Bollinger, J. M., Jr., and Krebs, C. (2006) Direct spectroscopic detection of a C-H-cleaving high-spin Fe(IV) complex in a prolyl-4-hydroxylase. *Proc. Natl. Acad. Sci. U.S.A.* **103**, 14738–14743.

(19) Lee, J. H., Bae, B., Kuemin, M., Circello, B. T., Metcalf, W. W., Nair, S. K., and van der Donk, W. A. (2010) Characterization and structure of DhpI, a phosphonate O-methyltransferase involved in dehydrophos biosynthesis. *Proc. Natl. Acad. Sci. U.S.A.* **107**, 17557–17562.

(20) Ogle, J. M., Clifton, I. J., Rutledge, P. J., Elkins, J. M., Burzlaff, N. I., Adlington, R. M., Roach, P. L., and Baldwin, J. E. (2001) Alternative oxidation by isopenicillin N synthase observed by X-ray diffraction. *Chem. Biol.* **8**, 1231–1237.

(21) Zhao, Z., Liu, P., Murakami, K., Kuzuyama, T., Seto, H., and Liu, H. W. (2002) Mechanistic Studies of HPP Epoxidase: Configuration of the Substrate Governs Its Enzymatic Fate. *Angew. Chem., Int. Ed.* **41**, 4529–4532.

(22) Yan, F., Moon, S. J., Liu, P., Zhao, Z., Lipscomb, J. D., Liu, A., and Liu, H. W. (2007) Determination of the substrate binding mode to the active site iron of (S)-2-hydroxypropylphosphonic acid epoxidase using ^{17}O -enriched substrates and substrate analogues. *Biochemistry* **46**, 12628–12638.